Polímeros
ISSN 1678-5169 (Online)

https://doi.org/10.1590/0104-1428.20240129

ORIGINAL ARTICLES

Production and physicochemical characterization of TEMPO-oxidized bacterial cellulose nanofibers from industrial waste*

Kely Silveira Bonfim[1]*, Daniella Lury Morgado[2], Renan da Silva Fernandes[1], Adhemar Watanuki Filho[1,3], Fauze Ahmad Aouada[1] and Márcia Regina de Moura[1]

[1]Grupo de Compósitos e Nanocompósitos Híbridos – GCNH, Departamento de Física e Química, Faculdade de Engenharia de Ilha Solteira – FEIS, Universidade Estadual Paulista "Júlio de Mesquita Filho" – UNESP, Ilha Solteira, SP, Brasil

[2]Departamento de Química, Universidade Federal de São Carlos – UFSCar, São Carlos, SP, Brasil

[3]Instituto Federal de São Paulo – IFS, Ilha Solteira, SP, Brasil

**This paper has been partially presented at the 17th Brazilian Polymer Congress, held in Joinville, SC, 29/Oct - 02/Nov/2023.*

**kely.s.bonfim@gmail.com*

Abstract

This study demonstrates the sustainable production and physicochemical characterization of nanofibers from bacterial cellulose (BC) waste generated during the commercial production of wound dressing films, using TEMPO-mediated oxidation. The produced BC nanofibers (TO-BCNF) were evaluated in terms of yield (82.68%) and water content (98.84%), and characterized by Transmission Electron Microscopy (TEM), Scanning Electron Microscopy (SEM), Fourier-Transform Infrared Spectroscopy (FTIR), X-Ray Diffraction (XRD), and Thermogravimetric Analysis (TGA). TEM revealed nanofibers with an average diameter of 116.07 ± 21.35 nm, while XRD confirmed the preservation of the semi-crystalline structure of BC, with a crystallinity index of 88.15%. TGA indicated thermal stability with degradation onset at 186 °C. The process also preserved the nanofibrillar morphology and the three-dimensional network of BC. This sustainable approach supports the circular bioeconomy by converting industrial waste into functional nanomaterials, offering potential for applications in wound dressings, films, hydrogels, and controlled release systems.

Keywords: *bio-based nanomaterials, nanofibrillated cellulose, circular bioeconomy, oxidative functionalization, biopolymer composites.*

Data Availability: Research data is available upon request from the corresponding author.

How to cite: Bonfim, K. S., Morgado, D. L., Fernandes, R. S., Watanuki Filho, A., Aouada, F. A., & Moura, M. R. (2025). Production and physicochemical characterization of TEMPO-oxidized bacterial cellulose nanofibers from industrial waste. *Polímeros: Ciência e Tecnologia*, *35*(4), e20250037 https://doi.org/10.1590/0104-1428.20240129

1. Introduction

In order to mitigate environmental effects and investigate substitutes for synthetic polymers has prompted materials scientists to focus more on finding novel and sustainable materials in recent years. In this context, biopolymers are promising sources for developing of novel materials and applications[1,2]. The most abundant biopolymer on Earth is cellulose $(C_6H_{10}O_5)_n$, a fundamental component of plant fibers, with an estimated annual production of 7.5×10^{10} tons per year[3,4]. Its linear, unbranched structure results from the condensation polymerization of anhydroglucose units joined by β-1,4 glycosidic bonds[5]. This homopolysaccharide exhibits high chain rigidity, it is insoluble in water, and is highly hygroscopic due to its free hydroxyl groups and hydrogen bonding[6].

Despite these properties, plant cellulose (PC) contains lignin, hemicellulose, and extractives, which require removal to obtain pure cellulose for technological applications. Extracting these components presents a significant challenge, given the intensive chemical processes that may compromise the material's sustainability[7]. Bacterial cellulose (BC), also known as biocellulose, has garnered significant attention from the scientific community due to its unique characteristics compared to PC. BC is biosynthesized by bacteria such as *Gluconacetobacter*, *Rhizobium*, *Sarcina*, *Agrobacterium,* and *Alcaligenes* in culture media containing fructose, glucose, sucrose, and xylose. This process results in a highly pure polymer, free from the other components typically found in PC, thus helping to reduce both environmental impacts and purification costs[8]. It must be pointed out that the dimensions and characteristics of the resulting materials are strongly influenced by both the origin of the cellulose and the specific conditions applied during extraction[9].

BC was first identified in 1886 during the vinegar fermentation[10]. It shares the same chemical composition as PC, but its fiber dimensions and structural organization differ[11], imparting unique properties: nano-scale fibers, high crystallinity, excellent mechanical and optical properties, flexibility, and the ability to form highly hydrated three-dimensional networks[12]. Due to these, BC has a wide range of including food packaging[13,14], the release of active materials[15,16], wound dressings[17,18], cosmetics[19,20], and electronics[21,22].

The increasing demand for sustainable materials has highlighted cellulose as a promising biopolymer. However, its intrinsic properties, such as limited mechanical strength and thermal resistance, restrict its applicability. Significant efforts have been undertaken to improve the properties of this material and expand its applications in composite synthesis and materials research. Nanostructured cellulose, such as nanofibers and nanocrystals, offers superior performance in advanced systems. Cellulose nanofibers (CNFs) differ markedly from cellulose nanocrystals (CNCs) in both structural features and potential applications. While the former nanomaterial is composed by long, thin fibers with lengths of up to 100 μm and diameters ranging from 3 to 100 nm[23] and the latter are shorter, rod-like particles obtained predominantly via strong acid hydrolysis, characterized by higher crystallinity and lower aspect ratios. CNCs show high crystallinity, aspect ratio, and excellent mechanical strength contribute significantly to the improvement of composite properties[4], notably in biodegradable polymers such as polylactic acid (PLA). For instance, Shi et al.[24] demonstrated that CNC incorporation into PLA substantially enhanced the mechanical performance of the biocomposite, broadening its potential for engineering plastic applications.

The investigation of cellulose nanofibers (CNFs) as a means of generating value from bacterial cellulose waste is supported by the fact that, although CNCs are well-established in the literature, CNFs have unique morphological and physicochemical characteristics that make them a flexible substitute. In particular, studies have increasingly focused on the nanostructures of bacterial cellulose, particularly its nanofibers[25,26]. In addition to their nanoscale dimensions, CNFs display a high surface area and the ability to form a highly porous network, both of which are essential properties for advanced applications in composite materials. Mechanical methods were the first employed in the disintegration of BC for the production of nanofibers. However, these methods have disadvantages, such as high energy consumption and equipment wear, limiting their viability on a large scale[27].

Chemical methods to obtain bacterial cellulose nanofibers (BCNF) include several strategies such as acid hydrolysis, alkali treatment, and oxidation reactions, such as TEMPO-oxidation. Acid hydrolysis is a widely employed method to break down cellulose fibers into smaller nanoparticles, while alkali treatment is often used to purify bacterial cellulose by removing any residual non-cellulosic impurities. However, acid hydrolysis lowers the crystallinity of cellulose fibers, affecting their mechanical and structural integrity. Furthermore, it exhibits poor selectivity, affecting both amorphous and crystalline areas. In contrast, alkali treatment successfully cleanses cellulose but does not introduce functional groups such as carboxylates, limiting its use. It may also modify the fiber surface, influencing how it interacts with other chemicals[28].

Alternatively, methods based on 2,2,6,6-tetramethyl-1-piperidinyloxyl (TEMPO)-mediated oxidation are well-established and widely used to produce bacterial cellulose nanofibers (TO-BCNF), offering advantages over these traditional approaches. In this process, the addition of sodium hypochlorite (NaClO) in the presence of catalytic amounts of TEMPO and sodium bromide (NaBr) at pH 10; facilitates the selective oxidation of the fibers. Specifically, the primary hydroxyl groups located at the C6 carbon of cellulose are first oxidized into aldehyde groups and subsequently converted into carboxylic acids. This chemical modification weakens the hydrogen bonds between fibrils, facilitating their disintegration into nanofibers. Moreover, the introduction of carboxylate groups not only improves the dispersibility of the fibers but also enables selective functionalization, thereby enhancing interactions with other materials[29-31]. These properties make TO-BCNF highly attractive for developing advanced nanocomposites, establishing the TEMPO method as a critical approach in materials chemistry. The literature includes numerous studies on TEMPO-mediated oxidation of bacterial cellulose[23,30-34]. In the field of dressings, BC is available as a form of film with pre-defined dimensions[35]. After the cutting process during commercial production of these dressings, the offcuts are discarded as waste and not reused. Utilizing this waste represents an innovative approach, promoting sustainability and contributing to the circular bioeconomy. Although few studies have explored industrial waste as a source of bacterial cellulose for BCNF production, further investigation is required[32-34,36-42].

Therefore, this study aimed to produce investigate the feasibility of utilizing industrial bacterial cellulose (BC) residues for the preparation of TEMPO-oxidized bacterial cellulose nanofibers (TO-BCNFs), without focusing on the optimization of the oxidation reaction conditions. We hypothesize that residual BC can be efficiently converted into high-quality nanofibers with structural and functional properties comparable to those from commercial BC. This strategy not only decreases the cost of manufacturing, but also improves sustainability by incorporating waste valorisation into nanocellulose production. The TEMPO-oxidation process was chosen because of its selectivity, which allows surface functionalization without affecting the crystalline structure, preserving the material's performance for advanced applications. The main objective was to assess how the selective oxidation of primary hydroxyl groups at the C6 position into carboxylate groups impacts the material's properties, while preserving its original crystalline structure and nanofibrillar morphology. Therefore, the obtained nanofibers were comprehensively characterized by X-ray diffraction (XRD), Fourier-transform infrared spectroscopy (FTIR), scanning electron microscopy (SEM), transmission electron microscopy (TEM), and thermogravimetric analysis (TGA). This approach not only promotes the valorization of biotechnological waste but also supports the development of advanced polymeric materials with potential applications such as wound dressings, films, hydrogels, and controlled release systems.

2. Materials and Methods

2.1 Materials

Bacterial cellulose (BC) scraps, originating from film-cutting operations during the manufacture of commercial dressings Nexfill®, Seven Indústria de Produtos Biotecnológicos Ltda), were generously supplied by the company and used as raw material in this study. 2,2,6,6-Tetramethylpiperidine-1-oxyl - TEMPO ($C_9H_{18}NO$) (CAS 2564-83-2, Sigma-Aldrich), sodium bromide (NaBr) (CAS 7647-15-6, Dinâmica), sodium hypochlorite 11% (NaClO) (CAS 7681-52-9, Dinâmica), sodium hydroxide (NaOH) (CAS 1310-73-2, Cinética) were used as received, without any purification. Deionized water (99% purity and electrical conductivity < 5 um.cm^{-2} - Reverse Osmosis ORBC-10A BFilters) was used for all experiments.

2.2 TEMPO-Mediated Oxidation

The oxidation of BC was carried out according to the method described in the literature[8], with some modifications. Briefly, 10 g of BC residues were homogenized and immersed in 1 L of an aqueous solution containing 0.16 g of 2,2,6,6-tetramethylpiperidine 1-oxyl and 1 g of NaBr. The oxidation reaction was initiated by adding NaClO (5.0 mmol.g^{-1} of dry CB). After the NaClO was fully consumed, the system's pH was maintained at 10.0 by dropwise adding a 0.5 mol.L^{-1} NaOH solution. The reaction system was mechanically stirred at 1000 rpm at room temperature for 2 hours. Upon completion of the oxidation, the suspension was sonicated for 10 minutes using a bath ultrasonicator (Unique Ultracleaner 1400), followed by filtration and washing with deionized water until the pH reached equal to 7.0. The remaining solids were subsequently fibrillated using a blender (Power L-22, Mondial) in seven cycles for 2 minutes each. The resulting material, being hereinafter referred to as TEMPO-oxidized bacterial cellulose nanofibers (TO-BCNF), was stored in a glass container under refrigeration for future analysis and applications.

2.3 Evaluation of dry matter yield after oxidation

The yield (Y) of TO-BCNF isolation via the TEMPO-mediated oxidation method was determined in triplicate based on the literature[43], using Equation 1, where: mf is the mass of TO-BCNF after drying in an oven at 100°C until constant weight; and mi is the dry mass of the BC residue used in the oxidation process.

$$Y(\%) = \left(\frac{mf}{mi}\right) \times 100 \quad (1)$$

2.4 Quantification of water content

The evaluation of water content of the TO-BCNF sample was determined in triplicate following the procedure described in the literature[44], using Equation 2, where: mi is the mass of TO-BCNF in suspension; and mf is the final mass of TO-BCNF after drying in an oven at 100 °C until constant weight.

$$Water\ Content(\%) = \left(\frac{mi - mf}{mi}\right) \times 100 \quad (2)$$

2.5 Electron Microscopy Characterization (SEM/TEM)

Nano- and microstructural analyses of BC and TO-BCNF samples were performed using scanning (SEM) and transmission (TEM) electron microscopy. Transmission Electron Microscopy (TEM) was used to characterize the morphology and size of the obtained TO-BCNFs. A diluted aqueous slurry containing TO-BCNF was dropped onto ultra-thin carbon-coated copper grids under ambient temperature and humidity. The sample was mounted in the of a TEM (TECNAI G2F20 - FEG) operated at 200 kV. The images were taken in conventional bright-field mode. The nanofiber diameter measurements were analyzed using ImageJ software, and the corresponding histograms were generated with OriginPro 9.

Scanning Electron Microscopy (SEM) was employed to evaluate the morphology and aggregation state of the TO-BCNFs after oxidation. The nanofibers suspension was freeze-dried at -55 ºC for 24 hours to preserve the structural integratiy of the material. The resulting material was mounted on an aluminum stub and coated with a thin layer of gold. Films samples (BC scraps) were used for BC analysis. Imaging was carried out using a scanning electron microscope (ZEISS, EVO/LS15) operated at an accelerating voltage of 10.0 kV.

2.6 Fourier Transform Infrared Spectroscopy (FT-IR)

The insertion of functional groups from TEMPO-mediated oxidation was qualitatively analyzed using attenuated total reflectance Fourier transform infrared spectroscopy (ATR-FTIR). BC and TO-BCNF samples, in the form of films, were placed in the sample holder of an Agilent Cary 630 spectrometer and subjected to 128 scans in the 4000 to 650 cm^{-1} range with a resolution of 4 cm^{-1} to obtain the spectra.

2.7 X-ray Diffraction (XDR)

The crystalline and semi-crystalline structures of the BC and TO-BCNF samples were analyzed using XRD analysis. The samples were placed in a glass sample holder of a Shimadzu-XRD-600 diffractometer with Cuα X-ray source (λ = 0,154 nm, a voltage of 30 kV, a current of 40 mA, an angular range (2θ) from 4° to 60°, and a 2°.min^{-1} scan rate). The crystallinity index (CrI) was determined following the literature[45] using the Segal equation (Equation 3), where: I_{200} is the maximum intensity (in arbitrary units) of the peak referring to the plane (200); and I_{am} is the diffraction intensity at 2θ = 18°.

$$CrI = \frac{(I_{200} - I_{am})}{I_{200}} \times 100 \quad (3)$$

2.8 Thermogravimetric analysis (TGA)

TGA analysis was performed using a thermal analyzer (TA Instruments SDT Q600 V20.9 Build 20). Prior to analysis, all samples were previously dried at 80 °C in an oven and subsequently stored in a desiccator. The samples, weighing approximately 8.0 mg and prepared as films, were placed in an aluminum sample holder and heated from room temperature to 800 °C, with a heating of 10 °C.min^{-1} under dynamic nitrogen atmosphere (100 mL.min^{-1}) Thermogravimetric curves were calculated using TA Instruments Advantage/ Universal Analysis (UA) software.

3. Results and Discussions

3.1 Yield and water content analysis

The yield of a process is an important metric used to identify losses that may occur during the conversion of a material into a final product. A thorough understanding of these losses is essential for optimizing the process and ensuring its effective implementation[46]. The yield of the BC waste oxidation process to produce TO-BCNF and the water content of the resulting material are presented in Table 1.

It can be seen that the oxidation process achieved a high yield, with only a 17.32% loss during the oxidation, sonication, filtration, washing, fibrillation and drying. This result shows that about 82.68% (Table 1) of the original bacterial cellulose mass was recovered as TO-BCNF. The observed mass loss can be attributed to the elimination of low-molecular-weight fractions, soluble byproducts produced during the oxidation reaction, and material losses caused by the nanofibrillation and purification phases. These results are consistent with those reported in the literature for oxidation processes using 5.0 mmol of NaClO, where yields of 89%[46] and 74%[47] were obtained. The result obtained for the yield of the oxidation reaction with TEMPO is satisfactory; however, it should be shown that the chemical reagents used, such as TEMPO and sodium bromide, contribute to the total cost of this type of reaction. In addition, it is worth mentioning that the raw material used in this study is an industrial waste material, thus supporting a more sustainable approach. The high water content of the produced TO-BCNF indicates its strong hydrophilic nature (Table 1). Quantifying the dry mass was essential for accurately determining the material's solid content, which is critical for reliable characterization, reproducibility of experimental conditions, and precise control of concentration-dependent properties in subsequent applications.

Table 1. Yield of the TEMPO-mediated oxidation process and water content of bacterial cellulose nanofibers.

Sample	Yield (%)	Water content (%)
TO-BCNF	82.68 ± 2.40	98.84 ± 0.07

3.2 Electron Microscopy Characterization (SEM/TEM)

Figure 1 shows the SEM and TEM images of the BC scraps and TO-BCNF obtained by TEMPO-mediated oxidation. The morphology of the BC nanofibers was assessed using SEM (Figure 1a and b) and TEM images (Figure 1c and d), which revealed a homogeneous three-dimensional network structure. The obtained TO-BCNF exhibited the characteristic appearance of long and thin, and tangled fibers, consistent with morphological features commonly reported for bacterial cellulose nanofibers in the literature[31,48-50]. A comparison between the micrographs of BC and TO-BCNF residues, as shown in Figure 1a-d, indicates that TEMPO-mediated oxidation did not alter the overall fibrillar morphology or network integrity of the material. However, the sonication process played a crucial role in promoting better dispersion of the nanofibrils, as the ultrasonic cavitation effect facilitates the breaking of chains in the amorphous regions[31,51]. Moreover, after oxidation, the anhydroglucose units may be cleaved, resulting in is the breakdown of cellulose into smaller nanofibrils[52].

The TO-BCNF produced in this study exhibited an average diameter of 116.07 ± 21.35 nm, within the typical range for nanofibers obtained via TEMPO-mediated oxidation. Song et al.[53] reported TOBCNs with an average diameter of ~80 nm, with such variations attributed to differences in source material, oxidation parameters, post-treatment conditions, and cellulose's physical state, particularly whether dried or never-dried[54]. Depending on these factors, more intense fibrillation and oxidation may be required to achieve specific morphological features; however, this can also generate fines and structural changes in the nanofibrillar network, potentially compromising its integrity and mechanical performance[55–57]. Notably, the optimal nanofiber diameter

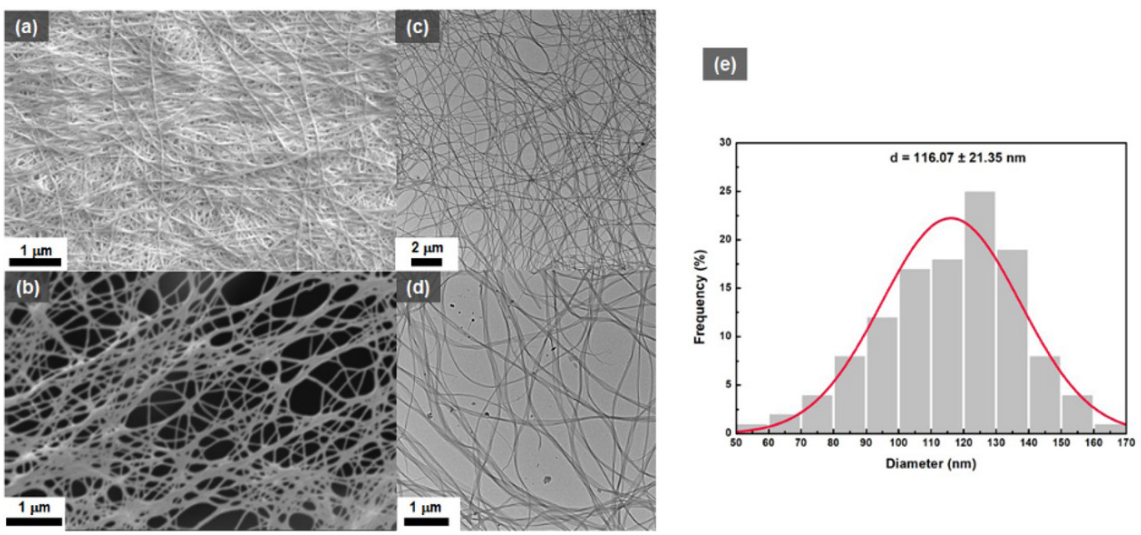

Figure 1. Morphological analysis: (a) SEM image of bacterial cellulose (BC); (b) SEM image of TEMPO-oxidized bacterial cellulose nanofibers (TO-BCNF); (c, d) TEM images of TO-BCNF at different magnifications; (e) average size and diameter distribution of bacterial cellulose nanofibers (TO-BCNF) based on TEM analysis.

depends on the intended application, as different fields require distinct specifications for mechanical properties and morphology. Overall, the TO-BCNF obtained here confirms that the adopted oxidation and sonication protocol effectively converted industrial BC residues into nanofibrils with consistent nanoscale features.

3.3 Fourier Transform Infrared Spectroscopy (FTIR)

Fourier-transform infrared (FTIR) spectra of BC and TO-BCNF samples were acquired in the range of 4000–600 cm^{-1}, as shown in Figure 2. The spectra of both BC and TO-BCNF (Figure 2) display characteristic absorption bands associated with the typical cellulose structure. The moderate intensity peak around 3324 cm^{-1} (Figure 2a) is attributed to O-H bond stretching vibrations, which is observed in both samples[21]. The peaks located at approximately 1160 and 1030 cm^{-1} (Figure 2c) corresponding to the asymmetric stretching vibrations of C-O-C linkages and the C-O stretching of secondary alcohols, respectively[21]. These peaks remain unchanged after oxidation, indicating that the cellulose polysaccharide backbone is preserved, and no significant degradation or disruption of the glycosidic linkages occurred. According to previous research, TEMPO-mediated oxidation primarily targets the principal hydroxyl groups (C6) while not altering the secondary hydroxyl groups (C2 and C3)[58]. The absorption at 2895 cm^{-1} (Figure 2a) is related to aliphatic C-H stretching, while the peak at 1370 is associated with C–H bending vibrations of the glucopyranose ring. The band at 1046 cm^{-1} (Figure 2b) is attributed to C–O stretching vibrations, mainly from C–OH and C–O–C linkages in the cellulose backbone[59].

It must be pointed out that the oxidation process applied to BC can be confirmed by FTIR analysis, primarily based on two key observations: (i) the appearance of a new absorption band at 1600 cm^{-1} in the TO-BNCF spectrum (Figure 2b), attributed to the asymmetric stretching vibration of carboxylate group ($-COO^-$), which is absent in the BC spectrum, and (ii) the lack of aldehyde-related bands in the 1720 – 1740 cm^{-1} region, indicating that the aldehyde groups (-CHO) were fully oxidized to carboxylate groups ($-COO^-$). This result indicates that the oxidation of primary hydroxyl groups at C6 occurred, although the carboxyl groups remain deprotonated under the current conditions. These results provide strong evidence for the selective oxidation of BC[46,60]. Moreover, TEMPO-mediated oxidation efficiently introduced carboxylate groups while preserving the nanofibrillar structure, as evidenced by SEM/TEM images and FTIR data, confirming the process's precision and reliability.

3.4 X-ray Diffraction (XDR)

XDR diffraction patterns of BC and TO-BCNF samples are presented in Figure 3, which confirm the semi-crystalline nature of both materials, with two main peaks. In the BC sample, characteristic diffraction peaks appear at 14.50° and 22.72°, corresponding to the (110) and (200) crystallographic planes of cellulose Iα, respectively[60]. These peaks indicate the highly crystalline structure of BC. Following TEMPO-mediated oxidation, the TO-BCNF sample maintained a similar diffraction pattern, confirming that the cellulose I polymorph was preserved. However, a slightly shifted to 14.68° and 22.86°, likely due to the introduction of carboxylate groups on the surface of cellulose I crystals, which could lead to subtle modifications in the inter-planar spacing[61].

The crystallinity index (CrI) of the samples was determined (Table 2), showing that both BC and TO-BCNF have a high degree of crystallinity. This result indicates that TEMPO-mediated oxidation does not significantly affect the crystalline structure of BC. It is likely that the carboxylate groups were primarily introduced at the surfaces of the crystallites and in the amorphous regions, rather than affecting the crystalline core[52,61,62]. These results clarify that, unlike plant-derived celluloses, which often show increased crystallinity after oxidation due to the removal of non-cellulosic amorphous components, such as lignin and hemicellulose, BC is already highly crystalline and essentially free of such impurities. Therefore, the TEMPO-mediated oxidation acted mainly on the accessible surfaces and amorphous regions without inducing recrystallization or significant reorganization of the crystalline domains. This explains the absence of a crystallinity increase despite the chemical modification[63].

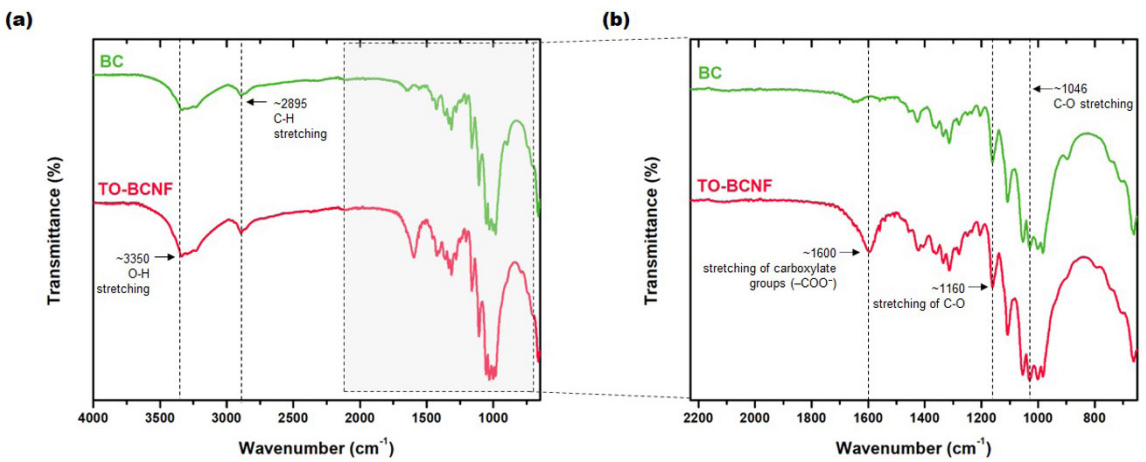

Figure 2. FTIR spectra of bacterial cellulose (BC) and TEMPO-oxidized bacterial cellulose nanofibers (TO-BCNF): (a) full spectral range (4000–655 cm^{-1}); (b) zoomed view of the 2232–655 cm^{-1} region.

These XRD data corroborate the FTIR results, indicating that TEMPO-mediated oxidation selectively changed the amorphous areas while leaving the crystalline cellulose domains intact. Notably, the structural properties of TO-BCNF generated from residual BC were equivalent to those frequently described for nanofibers derived from commercial BC, demonstrating the possibility of residual sources as a high-quality alternative.

3.5 Thermal properties

Thermogravimetric analysis (TGA) was performed to evaluate the thermal stability and degradation profile of BC and TO-BCNF samples. Figure 4 presents the thermogravimetric (TGA, Figure 4a) and derivative thermogravimetric (DTG, Figure 4b) curves of both materials, recorded from room temperature up to 800 °C. Both samples exhibit typical multi-step thermal degradation profiles, although TO-BCNF shows additional complexity due to surface modifications, as shown in Figure 4. The thermal analysis results were crucial for determining the initial (Ti), maximum (Tmax), and final (Tf) degradation temperatures, which are essential for understanding the material's stability. The mass loss at each stage further provides insight into the structural changes that occur during the heating process. BC exhibited two main stages of weight loss, and TO-BCNF exhibited three main stages (Table 3)

Table 2. Crystallinity Index for BC and TO-BCNF.

Sample	Crystallinity Index (%)
BC	89.52
TO-BCNF	88.15

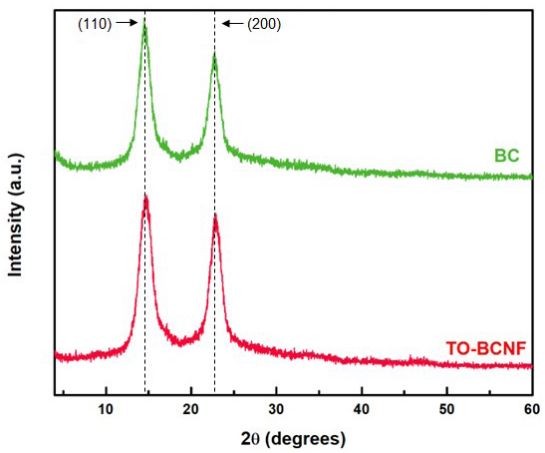

Figure 3. X-ray diffraction (XRD) patterns of BC and TO-BCNF, with indication of the crystallographic planes (110) and (200).

BC and TO-BCNF both exhibited an initial weight loss between 50 and 122 °C for BC and 68 and 116 °C for TO-BCNF, attributed to the evaporation of physically adsorbed water, which is a typical feature of hydrophilic cellulose materials[64]. Notably, TO-BCNF showed a slightly higher weight loss in this region compared to BC, reflecting its increased hydrophilicity due to the introduction of carboxylate groups during TEMPO-mediated oxidation. This modification enhances water retention by increasing the number of polar sites available for hydrogen bonding. These results confirm that oxidation not only alters the chemical structure but also significantly impacts the moisture affinity of the material. Although our TO-BCNF sample exhibited a high overall water content (98.84%, Table 1), both materials showed relatively low mass loss in the first thermal event (Table 3). This behavior is consistent with the known effects of cellulose drying. According to previous studies[54,65] drying induces hornification, leading to pore collapse and reduced accessibility to loosely bound water. Consequently, although dried cellulose can retain significant water structurally or through strong interactions, the amount of physically adsorbed water available for evaporation at low temperatures is limited. Therefore, the low water-related mass loss observed by TGA aligns with the structural characteristics of dried cellulose materials.

TO-BCNF demonstrated one additional thermal event compared to BC, emphasizing the oxidation process's impact on the material's thermal stability. Like BC, TO-BCNF also displayed a peak corresponding to the loss of water in the first stage. However, in the second and third stages, TO-BCNF showed two exothermic peaks, indicating cellulose breakdown following the oxidation process. These

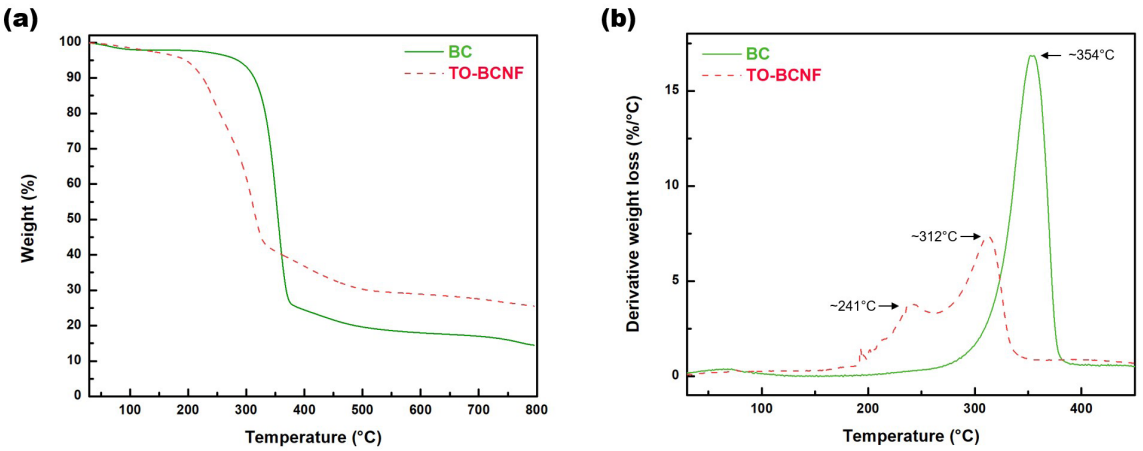

Figure 4. Thermal properties TGA (a) and DTG (b) of BC and TO-BCNF.

Table 3. Initial (Ti), Maximum (Tmax), and Final (Tf) temperatures, as well as the Mass Loss (%) for each thermal event of Bacterial Cellulose (BC) and Bacterial Cellulose Nanofibers (TO-BCNF).

Samples	1st thermal event				2nd thermal event				3rd thermal event			
	T_i (°C)	$T_{máx}$ (°C)	T_f (°C)	Mass Loss (%)	T_i (°C)	$T_{máx}$ (°C)	T_f (°C)	Mass Loss (%)	T_i (°C)	$T_{máx}$ (°C)	T_f (°C)	Mass Loss (%)
BC	50	65	122	2.2	224	354	398	73	-	-	-	-
TO-BCNF	68	74	116	2.0	186	241	263	18	263	312	361	37

findings indicate that the oxidation treatment not only adds carboxylate groups, but also alters the material's thermal characteristics, making it more prone to deterioration at higher temperatures than native BC. BC begins to degrade thermally at 224 °C, exhibiting a significant mass loss (73%, Table 3), at Tmax at 354 °C, related to cellulose degradation, dehydration and decomposition of glycosidic units[66]. In contrast, TO-BCNF shows its degradation event at a lower temperature of 186°C with a mass loss of 18% and the maximum thermal degradation temperature at 241°C, as shown in Table 3. This result indicates a reduction of 17% in thermal stability compared to BC[67].

This second thermal event for BC concluded at 398 °C, indicating a broad decomposition process typical of cellulose-based materials. In contrast, TO-BCNF shows its second thermal event at a lower temperature of 186 °C with a mass loss of 18% and the maximum thermal degradation temperature at 241 °C, as shown in Table 3. This event concluded at 263 °C, marking the end of the decomposition associated with the more labile amorphous regions of the oxidized nanofibers. The third thermal event of TO-BCNF was characterized by a 37% mass loss, occurring at a Tmax of 312 °C. This event initiated at 263 °C and finalized at 361 °C, corresponding to the progressive breakdown of partially crystalline domains and oxidized residues. This effect can be linked to the inclusion of carboxylate groups by TEMPO-mediated oxidation, which enhances the material's hydrophilicity while decreasing hydrogen bonding between cellulose strands. As a result, thermal degradation of the amorphous regions takes place at lower temperatures. The reduction in thermal stability is due to the insertion of these functional groups, which improve moisture retention and facilitate decarbonation processes, as reported in the literature. Previous research has shown that the thermal instability of TEMPO-oxidized cellulose is caused predominantly by the presence of thermally unstable anhydroglucuronate units, rather than glycosidic bond breakage or crystalline backbone degradation[68].

This interpretation is further reinforced by FTIR, XRD, SEM, and TEM results in this study, which collectively confirm the preservation of the polysaccharide backbone, the retention of cellulose I crystalline domains, and the maintenance of the nanofibrillar morphology after oxidation. Consequently, the additional thermal event observed in TO-BCNF is attributed to surface functionalization and increased chemical heterogeneity, rather than structural deterioration. The results shown here demonstrate that TEMPO-mediated oxidation lowers the thermal stability of BC, as previously reported in the literature[68,69]. Nonetheless, the TO-BCNF developed in this work has high heat resistance, with early degradation temperatures reaching 186 °C. Other investigations have shown similar results, with heat breakdown of oxidized BC beginning approximately 170 °C[70]. This suggests that, despite its early degradation onset, TO-BCNF has sufficient thermal resistance for applications requiring moderate stability. Additionally, valorising leftover BC enhances sustainability, offering a greener and more cost-effective alternative for cellulose-based nanomaterial production.

4. Conclusions

This work demonstrated the feasibility of repurposing industrial bacterial cellulose (BC) residue to generate nanofibers. The results showed that TEMPO-mediated oxidation can be employed as a strategic method aligned with circular bioeconomy principles, promoting both sustainability and industrial waste recovery. Furthermore, the produced bacterial cellulose nanofibers (TO-BCNF) exhibited high crystallinity and good thermal stability. The combination of TEMPO-mediated oxidation and fibrillation enabled the production of nanofibers with reduced diameters and improved dispersibility while preserving the semi-crystalline structure of BC. These properties highlight the potential of TO-BCNF as a high-performance functional material for advanced nanocomposites, with applications in wound dressings, films, hydrogels, and controlled release systems. This work contributes not only to the advancement of new polymeric materials but also to sustainable practices by repurposing bacterial cellulose waste, establishing it as a viable and valuable approach within the framework of the circular economy.

5. Author's Contribution

- **Conceptualization –** Kely Silveira Bonfim; Adhemar Watanuki Filho; Renan da Silva Fernandes; Márcia Regina de Moura.
- **Data curation –** Kely Silveira Bonfim.
- **Formal analysis –** Kely Silveira Bonfim; Daniella Lury Morgado.
- **Funding acquisition –** Márcia Regina de Moura; Fauze Ahmad Aouada.
- **Investigation –** Kely Silveira Bonfim.
- **Methodology –** Kely Silveira Bonfim; Adhemar Watanuki Filho; Renan da Silva Fernandes.
- **Project administration –** Kely Silveira Bonfim; Márcia Regina de Moura.
- **Resources –** Márcia Regina de Moura; Fauze Ahmad Aouada.
- **Software –** NA.

- **Supervision –** Márcia Regina de Moura; Fauze Ahmad Aouada.
- **Validation –** Kely Silveira Bonfim; Daniella Lury Morgado.
- **Visualization –** Kely Silveira Bonfim; Daniella Lury Morgado.
- **Writing – original draft –** Kely Silveira Bonfim; Adhemar Watanuki Filho; Renan da Silva Fernandes.
- **Writing – review & editing –** Kely Silveira Bonfim; Daniella Lury Morgado; Márcia Regina de Moura; Fauze Ahmad Aouada.

6. Acknowledgements

This research was funded by São Paulo State University (UNESP). São Paulo Research Foundation (FAPESP) (2019/06170-1; 2013/07296-2 – CEPID), and National Council for Scientific and Technological Development (CNPq) (MRM 408691/2023-9; 315513/2021-7; FAA 316174/2021-1; MCTIC Grant #406973/2022-9 through INCT/Polysaccharides - National Technology-Science Institute for Polysaccharides; and 307622/2023-1). This study was financed in part by the Coordenação de Aperfeiçoamento de Pessoal de Nível Superior - Brazil (CAPES) - "Finance Code 001", as well as grant numbers 88887.643328/2021-00 and 88887.712628/2022-00.

7. References

1. Getahun, M. J., Kassie, B. B., & Alemu, T. S. (2024). Recent advances in biopolymer synthesis, properties, & commercial applications: a review. *Process Biochemistry (Barking, London, England)*, *145*, 261-287. http://doi.org/10.1016/j.procbio.2024.06.034.
2. Islam, M. R., Rashid, M. N., Dev, B., Sayeed, M. Y., Alam, M. R., Mahmud, R. U., & Rahman, M. Z. (2024). *Progress in sustainable applications of polymers and biopolymers.* In S. Hashmi (Ed.), *Comprehensive materials processing* (pp. 523-554). USA: Elsevier. http://doi.org/10.1016/B978-0-323-96020-5.00212-0.
3. Suhas, G. V. K., Carrott, P. J. M., Singh, R., Chaudhary, M., & Kushwaha, S. (2016). Cellulose: a review as natural, modified and activated carbon adsorbent. *Bioresource Technology*, *216*, 1066-1076. http://doi.org/10.1016/j.biortech.2016.05.106. PMid:27265088.
4. Salleh, K. M., Selamat, M. E., Nordin, N. A., & Zuo, Q. (2025). Understanding nonwoody cellulose extractions, treatments, and properties for biomedical applications. *International Journal of Biological Macromolecules*, *308*(Pt 3), 142455. http://doi.org/10.1016/j.ijbiomac.2025.142455. PMid:40158602.
5. Channab, B.-E., El Idrissi, A., Essamlali, Y., & Zahouily, M. (2024). Nanocellulose: Structure, modification, biodegradation and applications in agriculture as slow/controlled release fertilizer, superabsorbent, and crop protection: a review. *Journal of Environmental Management*, *352*, 119928. http://doi.org/10.1016/j.jenvman.2023.119928. PMid:38219662.
6. Chashchilov, D. V. (2024). Regenerated Cellulose. Review. Part 1. Cellulose Structure, Solvent Systems, and Dissolution Mechanisms. *Polymer Science, Series D. Glues and Sealing Materials*, *17*(2), 466-473. http://doi.org/10.1134/S1995421224700801.
7. Islam, M. U., Ullah, M. W., Khan, S., Shah, N., & Park, J. K. (2017). Strategies for cost-effective and enhanced production of bacterial cellulose. *International Journal of Biological Macromolecules*, *102*, 1166-1173. http://doi.org/10.1016/j.ijbiomac.2017.04.110. PMid:28487196.
8. Viana, R. M., Sá, N. M. S. M., Barros, M. O., Borges, M. F., & Azeredo, H. M. C. (2018). Nanofibrillated bacterial cellulose and pectin edible films added with fruit purees. *Carbohydrate Polymers*, *196*, 27-32. http://doi.org/10.1016/j.carbpol.2018.05.017. PMid:29891296.
9. Jonoobi, M., Oladi, R., Davoudpour, Y., Oksman, K., Dufresne, A., Hamzeh, Y., & Davoodi, R. (2015). Different preparation methods and properties of nanostructured cellulose from various natural resources and residues: a review. *Cellulose (London, England)*, *22*(2), 935-969. http://doi.org/10.1007/s10570-015-0551-0.
10. Brown, A. J. (1886). XLIII.: on an acetic ferment which forms cellulose. *Journal of the Chemical Society Transactions*, *49*(0), 432-439. http://doi.org/10.1039/CT8864900432.
11. Du, R., Zhao, F., Peng, Q., Zhou, Z., & Han, Y. (2018). Production and characterization of bacterial cellulose produced by Gluconacetobacter xylinus isolated from Chinese persimmon vinegar. *Carbohydrate Polymers*, *194*, 200-207. http://doi.org/10.1016/j.carbpol.2018.04.041. PMid:29801830.
12. Pecoraro, É., Manzani, D., Messaddeq, Y., & Ribeiro, S. J. L. (2007). *Bacterial cellulose from glucanacetobacter xylinus: preparation, properties and applications*. In M. N. Belgacem, & A. Gandini, *Monomers, polymers and composites from renewable resources* (pp. 369-383). USA: Elsevier. https://www.doi.org/10.1016/B978-0-08-045316-3.00017-X.
13. Koreshkov, M., Takatsuna, Y., Bismarck, A., Fritz, I., Reimhult, E., & Zirbs, R. (2024). Sustainable food packaging using modified kombucha-derived bacterial cellulose nanofillers in biodegradable polymers. *RSC Sustainability*, *2*(8), 2367-2376. http://doi.org/10.1039/D4SU00168K.
14. Kusuma, A. C., Chou, Y.-C., Hsieh, C.-C., Santoso, S. P., Go, A. W., Lin, H.-T. V., Hsiao, I.-L., & Lin, S.-P. (2024). Agar-altered foaming bacterial cellulose with carvacrol for active food packaging applications. *Food Packaging and Shelf Life*, *42*, 101269. http://doi.org/10.1016/j.fpsl.2024.101269.
15. Sukhtezari, S., Almasi, H., Pirsa, S., Zandi, M., & Pirouzifard, M. (2017). Development of bacterial cellulose based slow-release active films by incorporation of Scrophularia striata Boiss. extract. *Carbohydrate Polymers*, *156*, 340-350. http://doi.org/10.1016/j.carbpol.2016.09.058. PMid:27842832.
16. Tsai, Y.-H., Yang, Y.-N., Ho, Y.-C., Tsai, M.-L., & Mi, F.-L. (2018). Drug release and antioxidant/antibacterial activities of silymarin-zein nanoparticle/bacterial cellulose nanofiber composite films. *Carbohydrate Polymers*, *180*, 286-296. http://doi.org/10.1016/j.carbpol.2017.09.100. PMid:29103507.
17. Kumineck, S. R. (2023). Development of bacterial cellulose incorporated with essential oils for wound treatment. *Polímeros: Ciência e Tecnologia*, *33*(4), e20230041. http://doi.org/10.1590/0104-1428.20230026.
18. Meng, S., Borjihan, Q., Xiao, D., Wang, Y., Chen, M., Cheng, C., & Dong, A. (2024). Biosynthesis of positively charged bacterial cellulose hydrogel with antibacterial and anti-inflammatory function for efficient wound healing. *International Journal of Biological Macromolecules*, *279*(Pt 3), 135263. http://doi.org/10.1016/j.ijbiomac.2024.135263. PMid:39244128.
19. Chantereau, G., Sharma, M., Abednejad, A., Vilela, C., Costa, E. M., Veiga, M., Antunes, F., Pintado, M. M., Sèbe, G., Coma, V., Freire, M. G., Freire, C. S. R., & Silvestre, A. J. D. (2020). Bacterial nanocellulose membranes loaded with vitamin B-based ionic liquids for dermal care applications. *Journal of Molecular Liquids*, *302*, 112547. http://doi.org/10.1016/j.molliq.2020.112547.
20. Amorim, J. D. P., & Galdino, C. J., Jr., Costa, A. F. S., Nascimento, H., Vinhas, G. M., & Sarubbo, L. A. (2020). BioMask, a polymer blend for treatment and healing of skin

prone to acne. *Chemical Engineering Transactions*, *79*, 205-210. https://doi.org/10.3303/CET2079035.

21. Zhang, T., Kuang, K., Lu, L., Li, Q., Sun, Y., & Miao, H. (2024). High strength bacterial cellulose/PANa-based hydrogel polyelectrolyte for flexible zinc−air batteries. *Journal of Energy Storage*, *100*(Pt B), 113629. https://doi.org/10.1016/j.est.2024.113629.
22. Saputra, A. M. A. (2025). Facile synthesis and electrochemical performance of bacterial cellulose/reduced graphene oxide/NiCo-layered double hydroxide composite film for self-standing supercapacitor electrode. *Materials Science for Energy Technologies*, *8*, 66-81. http://doi.org/10.1016/j.mset.2024.08.001.
23. Xu, H., Sanchez-Salvador, J. L., Blanco, A., Balea, A., & Negro, C. (2023). Recycling of TEMPO-mediated oxidation medium and its effect on nanocellulose properties. *Carbohydrate Polymers*, *319*, 121168. http://doi.org/10.1016/j.carbpol.2023.121168. PMid:37567710.
24. Shi, S.-C., Hsieh, C.-F., & Rahmadiawan, D. (2024). Enhancing mechanical properties of polylactic acid through the incorporation of cellulose nanocrystals for engineering plastic applications. *Teknomekanik*, *7*(1), 20-28. http://doi.org/10.24036/teknomekanik.v7i1.30072.
25. Adepu, S., Siju, C. R., Kaki, S., Bagannagari, S., Khandelwal, M., & Bharti, V. K. (2024). Review on need for designing sustainable and biodegradable face masks: opportunities for nanofibrous cellulosic filters. *International Journal of Biological Macromolecules*, *283*(Pt 2), 137627. http://doi.org/10.1016/j.ijbiomac.2024.137627. PMid:39547626.
26. Li, W., Yu, J., Li, Q., Wang, H., Liu, X., Li, P., Jiang, X., & Yang, J. (2024). Bacterial cellulose nanofiber reinforced self-healing hydrogel to construct a theranostic platform of antibacterial and enhanced wound healing. *International Journal of Biological Macromolecules*, *281*(Pt 2), 136336. http://doi.org/10.1016/j.ijbiomac.2024.136336. PMid:39370083.
27. Sofiah, A. G. N., Pasupuleti, J., Samykano, M., Kadirgama, K., Koh, S. P., Tiong, S. K., Pandey, A. K., Yaw, C. T., & Natarajan, S. K. (2023). Harnessing Nature's Ingenuity: a comprehensive exploration of nanocellulose from production to cutting-edge applications in engineering and sciences. *Polymers*, *15*(14), 3044. http://doi.org/10.3390/polym15143044. PMid:37514434.
28. Rostamabadi, H., Bist, Y., Kumar, Y., Yildirim-Yalcin, M., Ceyhan, T., & Falsafi, S. R. (2024). Cellulose nanofibers, nanocrystals, and bacterial nanocellulose: fabrication, characterization, and their most recent applications. *Future Postharvest and Food*, *1*(1), 5-33. http://doi.org/10.1002/fpf2.12001.
29. Nascimento, E. S., Pereira, A. L. S., Barros, M. O., Barroso, M. K. A., Lima, H. L. S., Borges, M. F., Feitosa, J. P. A., Azeredo, H. M. C., & Rosa, M. F. (2019). TEMPO oxidation and high-speed blending as a combined approach to disassemble bacterial cellulose. *Cellulose (London, England)*, *26*(4), 2291-2302. http://doi.org/10.1007/s10570-018-2208-2.
30. Saito, T., Kimura, S., Nishiyama, Y., & Isogai, A. (2007). Cellulose Nanofibers Prepared by TEMPO-Mediated oxidation of native cellulose. *Biomacromolecules*, *8*(8), 2485-2491. http://doi.org/10.1021/bm0703970. PMid:17630692.
31. Isogai, A., Saito, T., & Fukuzumi, H. (2011). TEMPO-oxidized cellulose nanofibers. *Nanoscale*, *3*(1), 71-85. http://doi.org/10.1039/C0NR00583E. PMid:20957280.
32. Rahmadiawan, D., Abral, H., Azka, M. A., Sapuan, S. M., Admi, R. I., Shi, S.-C., Zainul, R., Azril, A., Zikrii, A., & Mahardika, M. (2024). Enhanced properties of TEMPO-oxidized bacterial cellulose films via eco-friendly non-pressurized hot water vapor treatment for sustainable and smart food packaging. *RSC Advances*, *14*(40), 29624-29635. http://doi.org/10.1039/D4RA06099G. PMid:39297036.
33. Zhou, S., Peng, H., Zhao, A., Zhang, R., Li, T., Yang, X., & Lin, D. (2024). Synthesis of bacterial cellulose nanofibers/Ag nanoparticles: structure, characterization and antibacterial activity. *International Journal of Biological Macromolecules*, *259*(Pt 2), 129392. http://doi.org/10.1016/j.ijbiomac.2024.129392. PMid:38218289.
34. Ono, Y., Horikawa, Y., Takeuchi, M., Funada, R., & Isogai, A. (2024). Distribution of carboxy groups in TEMPO-oxidized cellulose nanofibrils prepared from never-dried Japanese cedar holocellulose, Japanese cedar-callus, and bacterial cellulose. *Cellulose (London, England)*, *31*(7), 4231-4245. http://doi.org/10.1007/s10570-024-05863-3.
35. Vuelo Pharma. (2024). *Membracel – Membrana Regeneradora Porosa*. Retrieved in 2024, November 29, from https://www.vuelopharma.com/membracel-porosa/
36. Chen, L., Lou, J., Rong, X., Liu, Z., Ding, Q., Li, X., Jiang, Y., Ji, X., & Han, W. (2023). Super-stretching and high-performance ionic thermoelectric hydrogels based on carboxylated bacterial cellulose coordination for self-powered sensors. *Carbohydrate Polymers*, *321*, 121310. http://doi.org/10.1016/j.carbpol.2023.121310. PMid:37739507.
37. Wang, F., Kim, H.-J., Park, S., Kee, C.-D., Kim, S.-J., & Oh, I.-K. (2016). Bendable and flexible supercapacitor based on polypyrrole-coated bacterial cellulose core-shell composite network. *Composites Science and Technology*, *128*, 33-40. http://doi.org/10.1016/j.compscitech.2016.03.012.
38. Chitbanyong, K., Pisutpiched, S., Khantayanuwong, S., Theeragool, G., & Puangsin, B. (2020). TEMPO-oxidized cellulose nanofibril film from nano-structured bacterial cellulose derived from the recently developed thermotolerant Komagataeibacter xylinus C30 and Komagataeibacter oboediens R37–9 strains. *International Journal of Biological Macromolecules*, *163*, 1908-1914. http://doi.org/10.1016/j.ijbiomac.2020.09.124. PMid:32976905.
39. Wang, X., Tang, S., Chai, S., Wang, P., Qin, J., Pei, W., Bian, H., Jiang, Q., & Huang, C. (2021). Preparing printable bacterial cellulose based gelatin gel to promote in vivo bone regeneration. *Carbohydrate Polymers*, *270*, 118342. http://doi.org/10.1016/j.carbpol.2021.118342. PMid:34364595.
40. Wang, K., Hazra, R. S., Ma, Q., Jiang, L., Liu, Z., Zhang, Y., Wang, S., & Han, G. (2022). Multifunctional silk fibroin/PVA bio-nanocomposite films containing TEMPO-oxidized bacterial cellulose nanofibers and silver nanoparticles. *Cellulose (London, England)*, *29*(3), 1647-1666. http://doi.org/10.1007/s10570-021-04369-6.
41. Ono, Y., Takeuchi, M., Kimura, S., Puangsin, B., Wu, C.-N., & Isogai, A. (2022). Structures, molar mass distributions, and morphologies of TEMPO-oxidized bacterial cellulose fibrils. *Cellulose (London, England)*, *29*(9), 4977-4992. http://doi.org/10.1007/s10570-022-04617-3.
42. Wu, C.-N., Fuh, S.-C., Lin, S.-P., Lin, Y.-Y., Chen, H.-Y., Liu, J.-M., & Cheng, K.-C. (2018). TEMPO-Oxidized Bacterial Cellulose Pellicle with Silver Nanoparticles for Wound Dressing. *Biomacromolecules*, *19*(2), 544-554. http://doi.org/10.1021/acs.biomac.7b01660. PMid:29334612.
43. Moussa, I., Khiari, R., Moussa, A., Belgacem, M. N., & Mhenni, M. F. (2019). Preparation and characterization of carboxymethyl cellulose with a high degree of substitution from agricultural wastes. *Fibers and Polymers*, *20*(5), 933-943. http://doi.org/10.1007/s12221-019-8665-x.
44. Fischer, M. R., Garcia, M. C. F., Nogueira, A. L., Porto, L. M., Schneider, A. L. S., & Pezzin, A. P. T. (2018). Biossíntese e caracterização de nanocelulose bacteriana para engenharia de tecidos. *Matéria (Rio de Janeiro)*, *22*(suppl 1), 22. http://doi.org/10.1590/s1517-707620170005.0270.
45. Segal, L., Creely, J. J., Martin, A. E., Jr., & Conrad, C. M. (1959). An empirical method for estimating the degree of crystallinity of native cellulose using the X-Ray Diffractometer. *Textile Research Journal*, *29*(10), 786-794. http://doi.org/10.1177/004051755902901003.

46. Nascimento, E. S. (2018). *Filmes nanocompósitos à base de celulose bacteriana e nanocristais de celulose* (Doctoral dissertation). Universidade Federal do Ceará, Fortaleza. Retrieved in 2024, November 29, from https://repositorio.ufc.br/handle/riufc/34774
47. Nunes, T. F. G. (2014). *Produção, caracterização e aplicação de nanofibras de celulose* (Master's thesis). Faculdade de Ciências e Tecnologia, Universidade de Coimbra, Portugal. Retrieved in 2024, November 29, from https://hdl.handle.net/10316/30004
48. Liu, Z., Lin, D., Lopez-Sanchez, P., & Yang, X. (2020). Characterizations of bacterial cellulose nanofibers reinforced edible films based on konjac glucomannan. *International Journal of Biological Macromolecules*, *145*, 634-645. http://doi.org/10.1016/j.ijbiomac.2019.12.109. PMid:31857167.
49. Zhai, X., Lin, D., Liu, D., & Yang, X. (2018). Emulsions stabilized by nanofibers from bacterial cellulose: new potential food-grade Pickering emulsions. *Food Research International*, *103*, 12-20. http://doi.org/10.1016/j.foodres.2017.10.030. PMid:29389597.
50. Chen, Y., Chen, S., Wang, B., Yao, J., & Wang, H. (2017). TEMPO-oxidized bacterial cellulose nanofibers-supported gold nanoparticles with superior catalytic properties. *Carbohydrate Polymers*, *160*, 34-42. http://doi.org/10.1016/j.carbpol.2016.12.020. PMid:28115098.
51. Zanon, C. D. (2016). *Produção de nanocompósitos obtenção de nanofibras de celulose de folhas de bananeira via oxidação catalítica* (Master's thesis). Universidade Estadual de Campinas, Campinas. https://www.doi.org/10.47749/T/UNICAMP.2016.971491.
52. Li, L., Chen, Y., Yu, T., Wang, N., Wang, C., & Wang, H. (2019). Preparation of polylactic acid/TEMPO-oxidized bacterial cellulose nanocomposites for 3D printing via Pickering emulsion approach. *Composites Communications*, *16*, 162-167. http://doi.org/10.1016/j.coco.2019.10.004.
53. Song, J. E., Jun, S.-H., Park, S.-G., & Kang, N.-G. (2020). A semi-dissolving microneedle patch incorporating TEMPO-oxidized bacterial cellulose nanofibers for enhanced transdermal delivery. *Polymers*, *12*(9), 1873. http://doi.org/10.3390/polym12091873. PMid:32825232.
54. Saito, T., Nishiyama, Y., Putaux, J.-L., Vignon, M., & Isogai, A. (2006). Homogeneous suspensions of individualized microfibrils from TEMPO-Catalyzed oxidation of native cellulose. *Biomacromolecules*, *7*(6), 1687-1691. http://doi.org/10.1021/bm060154s. PMid:16768384.
55. Levanič, J., Šenk, V. P., Nadrah, P., Poljanšek, I., Oven, P., & Haapala, A. (2020). Analyzing TEMPO-Oxidized cellulose fiber morphology: new insights into optimization of the oxidation process and nanocellulose dispersion quality. *ACS Sustainable Chemistry & Engineering*, *8*(48), 17752-17762. http://doi.org/10.1021/acssuschemeng.0c05989.
56. Wang, M., Miao, X., Li, H., & Chen, C. (2021). Effect of length of cellulose nanofibers on mechanical reinforcement of polyvinyl alcohol. *Polymers*, *14*(1), 128. http://doi.org/10.3390/polym14010128. PMid:35012151.
57. Kafy, A., Kim, H. C., Zhai, L., Kim, J. W., Van Hai, L., Kang, T. J., & Kim, J. (2017). Cellulose long fibers fabricated from cellulose nanofibers and its strong and tough characteristics. *Scientific Reports*, *7*(1), 17683. http://doi.org/10.1038/s41598-017-17713-3. PMid:29247191.
58. Jun, S.-H., Park, S.-G., & Kang, N.-G. (2019). One-pot method of synthesizing TEMPO-oxidized bacterial cellulose nanofibers using immobilized TEMPO for skincare applications. *Polymers*, *11*(6), 1044. http://doi.org/10.3390/polym11061044. PMid:31197111.
59. Yang, Y.-N., Lu, K.-Y., Wang, P., Ho, Y.-C., Tsai, M.-L., & Mi, F.-L. (2020). Development of bacterial cellulose/chitin multi-nanofibers based smart films containing natural active microspheres and nanoparticles formed in situ. *Carbohydrate Polymers*, *228*, 115370. http://doi.org/10.1016/j.carbpol.2019.115370. PMid:31635728.
60. Ye, J., Li, J., Wang, X., Wang, Q., Wang, S., Wang, H., Zhu, H., & Xu, J. (2024). Preparation of bacterial cellulose-based antibacterial membranes with prolonged release of drugs: emphasis on the chemical structure of drugs. *Carbohydrate Polymers*, *323*, 121379. http://doi.org/10.1016/j.carbpol.2023.121379. PMid:37940275.
61. Saito, T., & Isogai, A. (2004). TEMPO-Mediated oxidation of native cellulose. The effect of oxidation conditions on chemical and crystal structures of the water-insoluble fractions. *Biomacromolecules*, *5*(5), 1983-1989. http://doi.org/10.1021/bm0497769. PMid:15360314.
62. Fu, R., Ren, Y., Fang, K., Sun, Y., Zhang, Z., & Luo, A. (2021). Preparation, Characterization and Biocompatibility of Chitosan/TEMPO-oxidized bacterial cellulose composite film for potential wound dressing applications. *Fibers and Polymers*, *22*(7), 1790-1799. http://doi.org/10.1007/s12221-021-0854-8.
63. Pratama, A. W., Piluharto, B., Mahardika, M., Widiastuti, N., Firmanda, A., & Norrrahim, M. N. F. (2024). Comparative study of oxidized cellulose nanofibrils properties from diverse sources via TEMPO-mediated oxidation. *Case Studies in Chemical and Environmental Engineering*, *10*, 100823. http://doi.org/10.1016/j.cscee.2024.100823.
64. Vasconcelos, N. F., Cunha, A. P., Ricardo, N. M. P. S., Freire, R. S., Vieira, L. A. P., Santa Brígida, A. I., Borges, M. de F., Rosa, M. F., Vieira, R. S., & Andrade, F. K. (2020). Papain immobilization on heterofunctional membrane bacterial cellulose as a potential strategy for the debridement of skin wounds. *International Journal of Biological Macromolecules*, *165*(Pt B), 3065-3077. http://doi.org/10.1016/j.ijbiomac.2020.10.200. PMid:33127544.
65. Spinu, M., Santos, N., Le Moigne, N., & Navard, P. (2011). How does the never-dried state influence the swelling and dissolution of cellulose fibres in aqueous solvent? *Cellulose (London, England)*, *18*(2), 247-256. http://doi.org/10.1007/s10570-010-9485-8.
66. Gaulke, E., Garcia, M. C. F., Segat, B., Apati, G. P., Schneider, A. L. S., Pezzin, A. P. T., Cesca, K., & Porto, L. M. (2023). Evaluation of potential biomaterials for application in guide bone regeneration from Bacterial nanocellulose/Hydroxyapatite. *Polímeros: Ciência e Tecnologia*, *33*(3), e20230034. http://doi.org/10.1590/0104-1428.20220121.
67. Nóvak, I. C., Segat, B., Garcia, M. C. F., Pezzin, A. P. T., & Schneider, A. L. S. (2024). Alternative production of bacterial cellulose by Komagataeibacter hansenii and microbial consortium. *Polímeros: Ciência e Tecnologia*, *34*(2), e20240021. http://doi.org/10.1590/0104-1428.20230080.
68. Fukuzumi, H., Saito, T., Okita, Y., & Isogai, A. (2010). Thermal stabilization of TEMPO-oxidized cellulose. *Polymer Degradation & Stability*, *95*(9), 1502-1508. http://doi.org/10.1016/j.polymdegradstab.2010.06.015.
69. Jayani, T., Sanjeev, B., Marimuthu, S., & Uthandi, S. (2020). Bacterial Cellulose Nano Fiber (BCNF) as carrier support for the immobilization of probiotic, Lactobacillus acidophilus 016. *Carbohydrate Polymers*, *250*, 116965. http://doi.org/10.1016/j.carbpol.2020.116965. PMid:33049863.
70. Wen, Y., Liu, J., Jiang, L., Zhu, Z., He, S., He, S., & Shao, W. (2021). Development of intelligent/active food packaging film based on TEMPO-oxidized bacterial cellulose containing thymol and anthocyanin-rich purple potato extract for shelf life extension of shrimp. *Food Packaging and Shelf Life*, *29*, 100709. http://doi.org/10.1016/j.fpsl.2021.100709.

Received: Feb. 08, 2025
Revised: May 28, 2025
Accepted: Jun. 09, 2025

Associate Editor: César L. Petzhold